Investigating the effects of wheel/rail surface roughness on wheel/rail wear

A. Shebani
College of Computer Technology – Zawya
amershebani@gmail.com

Abstract

Wear can be defined as the removal of material from solid surfaces by mechanical action. Wheel/rail wear is an everyday experience, and has been observed and studied for a very long time. Many railway accidents have occurred that were related to poor maintenance and wheel/rail wear. Therefore, there is a need to study the wheel and rail wear, so as to make informed decisions on wheel and rail maintenance, and reduce maintenance costs. This work focus on investigate the relationship between the wheel/rail surface roughness and wheel/rail wear. To study the relationship between the wheel/rail roughness parameters and the wheel/rail wear, a twin disc rig test and Alicona profilometer were used. This study can use to eliminate the wheel/rail wear and improve the design of the wheel and rail. This paper presented an Alicona profilometer and replica material as an effective tool to study the wheel/rail surface texture.

Keywords: wheel wear, rail wear, roughness, Alicona profilometer, replica material, twin disc rig test.

1. Introduction

1.1 Surface texture (Roughness and waviness)

Surface texture is an important issue when the main interest is to understand the nature of material surfaces and it plays an important role in the functional performance of many engineering components [1]. When two nominally rough surfaces are placed in contact, surface roughness causes contact to occur at discrete contact spots (junctions) such as in Figure:. (1). Then sum of the areas of all the contact spots constitutes the real (true) area of contact or simply contact area, and for most materials with applied load, this will be only a small fraction of the apparent (nominal) area of contact (that which would occur if the surfaces were perfectly smooth). The real area of contact is a function of the surface texture, material properties and interfacial loading conditions. The proximity of the asperities results in adhesive contacts caused by interatomic interactions. During the contact of two surfaces, contact will initially occur at only a few points to support the normal load (force). As the normal load is increased, the surfaces move closer together, a large number of higher asperities on the two surfaces come into contact, and existing contacts grow to support the increasing load. Deformation occurs in the region of the contact spots, establishing stresses that oppose the applied load. The mode of the surface deformation may be elastic, or plastic, and depends on nominal normal shear stresses (apparent contact area), surface roughness, and material properties [2].

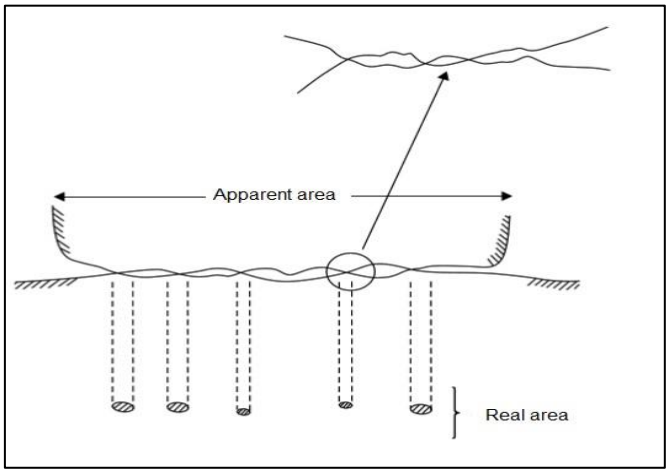

Figure: 1 Apparent area and real area [2]

All surfaces are rough on a microscopic scale, and when the two rough surfaces are in contact the real area is very small compared to the apparent area of the contact. When loading presses two rough surfaces together, only some peaks of the surfaces will be in contact such as in Figure 2 [3].

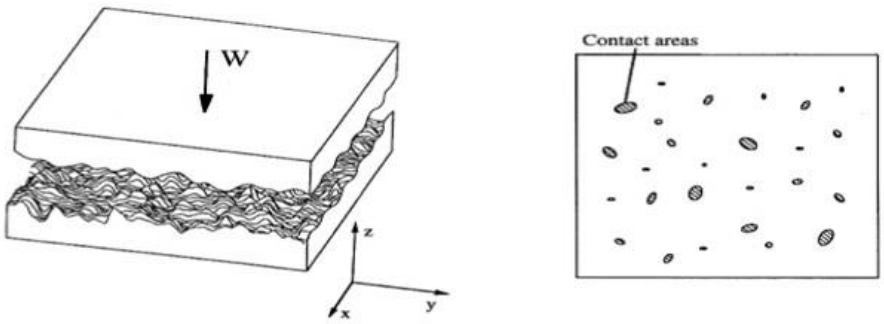

Figure: 2 Schematic of the real area of contact [3]

1.2 Analysis of surface roughness

Surface texture is the repetitive or random deviation from the nominal surface that forms the three-dimensional topography of the surface. Surface texture includes: roughness (nanoroughness), waviness (macroroughness), lay, and flaws. Nano- and macroroughness are formed by fluctuations in the surface of short wavelengths, characterized by hills (asperities) and valleys of varying amplitudes and spacing, and these are large compared to molecular dimensions. Asperities are referred to as peaks in a profile (two dimensions) and summits in a surface map (three dimensions). Figure 3 shows the surface roughness and waviness [4].

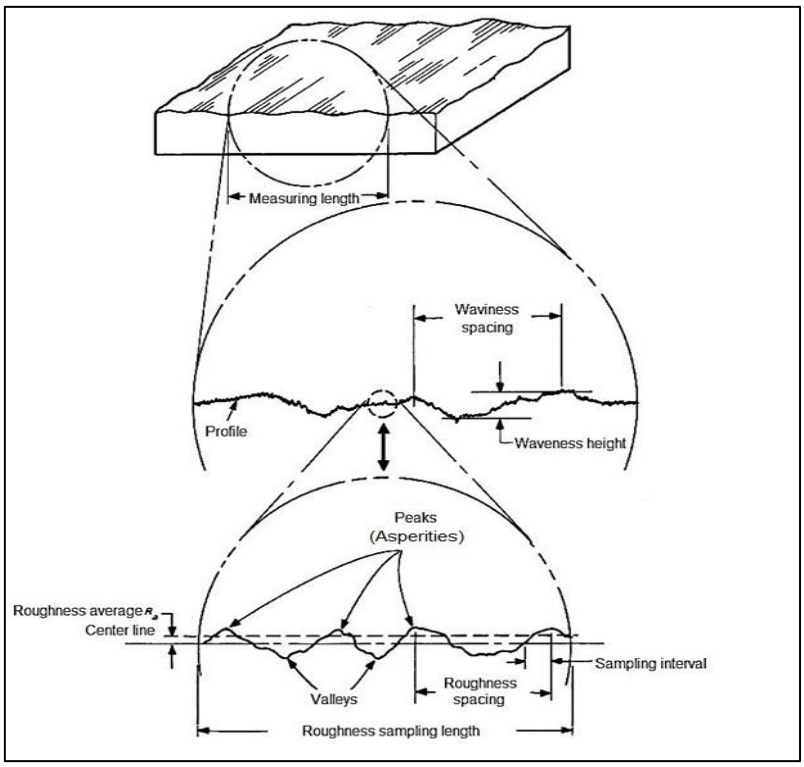

Figure: 3 Surface roughness and waviness [4]

Figure 4 shows the original profile, waviness profile, and roughness profile

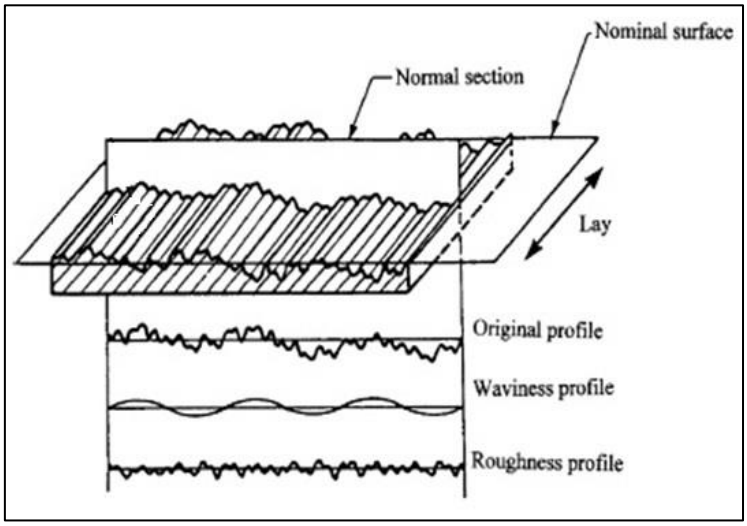

Figure: 4 Original profile, waviness profile, and roughness profile [5]

1.3 Basic definitions in roughness surface

- Surface: The surface of an object is the boundary which separates that object from another substance. Its shape and extent are usually defined by a drawing or descriptive specifications [6].
- Profile, it can be defined It is the contour of any specified section through a surface [6].
- Nominal surface, it is the intended surface. The shape and extent of a nominal surface are usually shown and dimensioned on a drawing. The nominal surface does not include intended surface roughness [7].
- A real surface is the actual boundary of an object. It deviates from the nominal surface as a result of the process that created

the surface. The deviation also depends on the properties, composition, and structure of the material the object is made of [7].

- Measured profile can be defined as the profile obtained with some measuring profilometer [8].
- Nominal profile is the straight or the smoothly line of intersection of the nominal surface with a plan which perpendicular to the surface [8].
- Primary profile is the sum of all the deviations of the measured profile from the nominal profile [8].
- Waviness profile is a recurrent deviation from a flat surface, much like waves on the surface of water [6].
- Roughness profile is defined as closely spaced, irregular deviations on a scale smaller than that of waviness. Roughness is expressed in terms of its height, its width, and its distance on the surface along which it is measured [6].
- Lay, it is referring to the predominant direction of the surface texture. Ordinarily lay is determined by the particular production method and geometry used [7].

1.4 Profile Filter

Filters play a fundamental role in the analysis of surface texture measurement. It is the process of extracting, or suppressing, certain wavelengths or spatial frequencies in the total profile, for example the attempts to reduce the effects of instrument noise and imperfections. The Profile filter is the filter that separates profiles into longwave and shortwave components. There are three filters used in instruments for measuring surface roughness, waviness and primary profiles. They all possess the same transmission characteristics, but have differing cut-off wavelengths such as in Figure 5 [9].

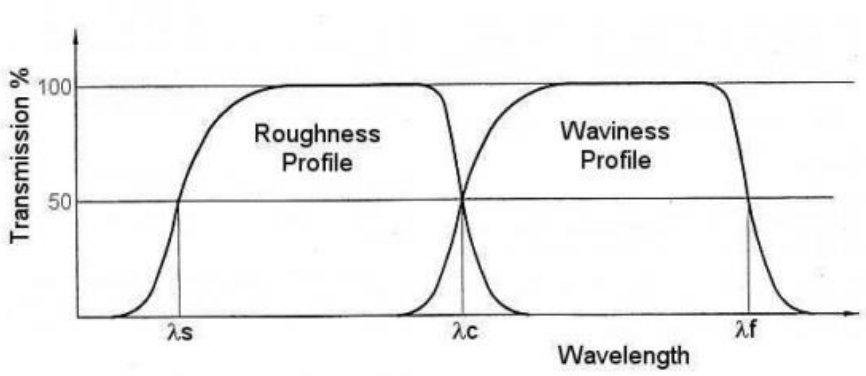

Figure: 5 Transmission characteristic of roughness and waviness profiles [9]

λs Profile Filter This is the filter that defines the intersection between the roughness and shorter wave components, such as instrument noise, present in a surface [9].

λc Profile Filter This is the filter that defines the intersection between the roughness and waviness components [9].

λf Profile Filter This is the filter that defines the intersection between the waviness and longer wave components, such as form, present in a surface [9].

1.5 Roughness parameters

Roughness average (R_a), it called centre line average value or arithmetic average. Among Height Parameters, the roughness average (Ra) is the most widely used because it is a simple parameter to obtain when compared to others. The roughness average is described as follows [1]:

$$R_a = \frac{1}{L} \int_0^L |Z(x)| \quad (33)$$

Where $Z(x)$ is the function that describes the surface profile analyzed in terms of height (Z) and position (x) of the sample over the evaluation length "L" Figure 6.

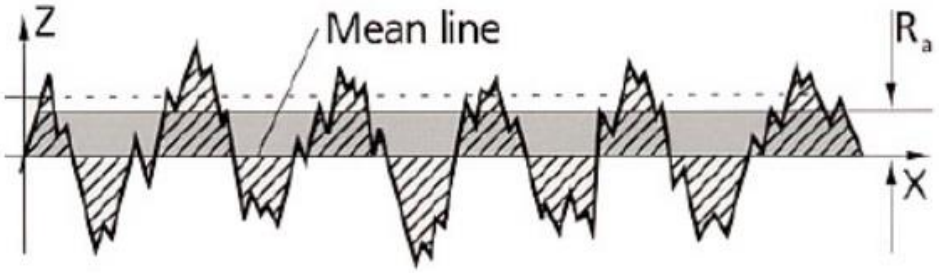

Figure: 6 Profile of a surface (Z). It represents the average roughness Ra [1]

2. Surface Measuring

2.1 Introduction

It is essential to consistently measure the surface roughness of work pieces as broad definitions of 'smooth surface' or 'rough surface' are inadequate. The ideal method by which to characterize surface roughness is through direct measurement with an appropriate tool. In this context surface roughness is usually quantified by the vertical deviations of a surface from its mean profile. Historically, the stylus instrument was the most widely accepted method to measure surface roughness as it gave more accurate results compared to other methods. Presently, many surface measuring instruments are used in manufacturing. For example, stylus instruments are widely used in the automotive industry, while optical instruments are often used in manufacturing where a non-contact method is required. Optical instruments do not make contact with surfaces and thus do not leave

any trace or damage. Surface measuring instruments currently used in manufacturing can be sorted into two groups as follows [10].

2.2 Non-Contact approach

Optical profilometer measures surface roughness by using the laws of reflection as shown in Figure:. (7). Instruments that use this technique make use of focus detection, interferometry, and projected light. The optical interference method is suitable for measuring roughness of soft materials which are easily damaged. It is widely used in manufacturing of lenses and hard disk equipment [10].

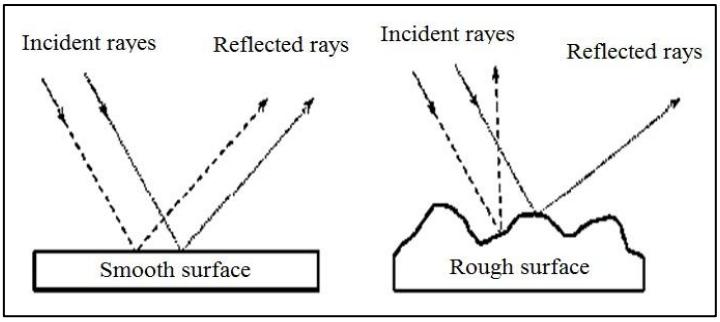

Figure: 7 Representative scheme for reflecting of light with smooth and rough surfaces [10]

Figure 8 shows the schematic of the optical surface profile. The main idea of the optical interference instrument is to identify the wavelengths of the light beams that are reflected from the test material and the reference mirror. Both wavelengths of the light beam will be used to calculate the height differences over a surface profile [10].

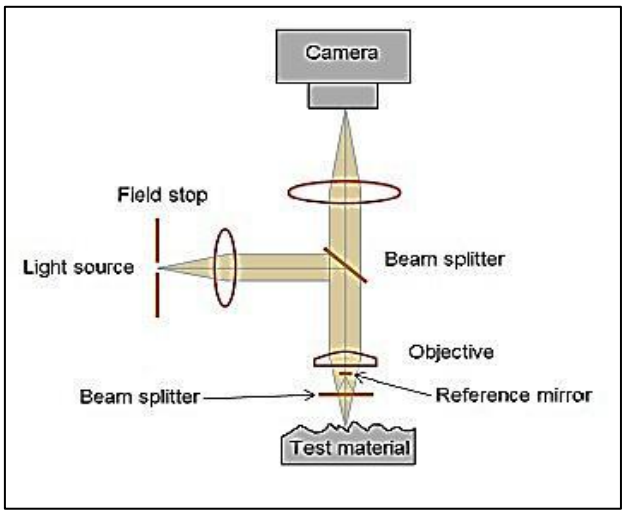

Figure: 8 Schematic of the optical surface profile [10]

2.3 Contact approach

Surface profilometer, also known as the 'Stylus method', is operated by moving a stylus along a surface. The stylus moves up and down following the peaks or valleys in the surface, and records this in terms of Cartesian coordinates as shown in Figure:. (9) [10].

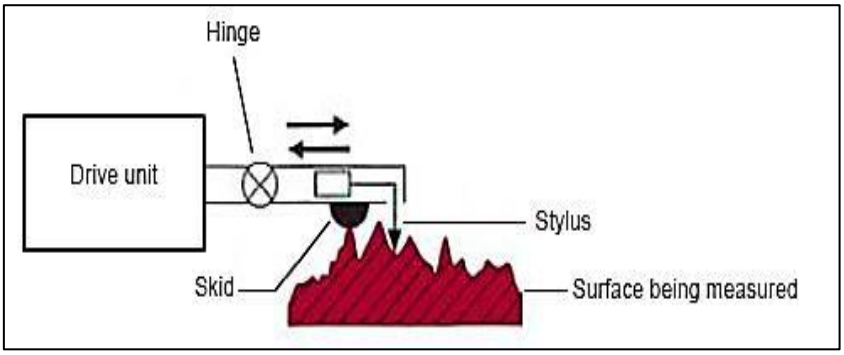

Figure: 9 Schematic of the working principle of a stylus profilometer [10]

The stylus technique which is the most commonly used class of surface texture measuremens instrument. Figure:ure:. (10) shows a schematic diagram of a stylus instrument. The stylus traverses the surface peaks and valleys, and the vertical motion of the stlus is converted by the transducer into an electrical signal which may be analyzed by digital or analog techniques. In many kinds of modern instruments, the signal undergoes analog-to-digital conversion. The resulting digital profile is stored in a computer and canbe anlyzed subseqeuntly for roughness parameters [11].

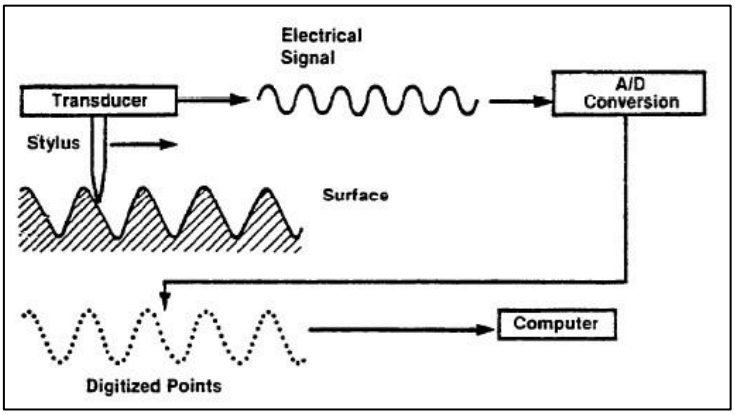

Figure: 10 Schematic diagram of stylus instrument [11]

Figure 11 shows a schematic diagram of a stylus transducer, this transducer is called a linear variable differential transformer (LVDT). The stylus is fastened to a ferrite core, which is positioned between two coils that form part of an AC bridge. As ferrite core moves up and down between the coils, the balance of the bridge is changed. The resulting output, after suitable demodulation and amplification, is a voltage signal that is proportional to the displacement of the stylus. The output of the LVDT, therefore, is directly proportional to surface height and hence yields the profile as the surface is scanned [11].

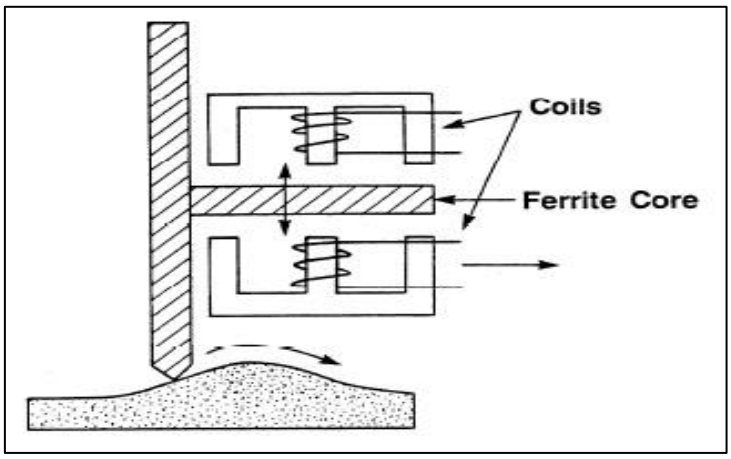

Figure: 11 Schematic diagram of LVDT transducer [11]

3. Wheel and rail wear

Due to the importance of the wheel and rail wear issue which is related to safety and economy, many experimental tests were carried out in this work using the twin disc rig to investigate the effects of some important parameters such as load, yaw angle, and speed on the wheel/rail wear under dry conditions. Figure: (12) shows the wheel/rail wear positions which is needs to be measured in this project (wheel wear and rail wear).

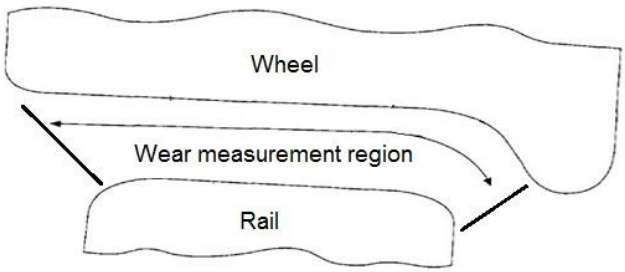

Figure: 12 Wheel and rail wear

The twin-disc system is simple and efficient; it consists of the use of two rollers pressed into contact, the variation of the relative velocity and of the contact pressure allows performing of the test under different conditions [12]. The twin disc approach has been shown to provide a good approach for comparing adhesion levels under a range of wheel/rail contact conditions, with and without contaminants [13]. Twin disc wear testing, used extensively for studying wear of wheel and rail materials [14].

The twin disc rig used in this work consists of an upper steel wheel of 310mm diameter and a lower steel wheel with diameter of 290mm. The rollers and shafts are made of EN24T steel. Vertical force of up to 4KN can be applied on the rollers through a jacking mechanism. The rig consists of a rotary table to allow a relative yaw angle between the rollers; this yaw angle is indicated by markings on the handle of the rotary table. In this work the replica technique used for wear and roughness measurements of the twin disc rollers, where the replica used to make a copy of the wheel/rail surfaces of two rollers before the test and after each test, and then the Alicona profilometer used to measure the wheel/rail wear. The name of the replica material which is used in this work is AccuTrans [15].

The Alicona profilometer generates the wheel/rail roughness profiles using different filters such as in a standard ISO 2478 [16].

The Alicona profilometer (INFINTE FOCUS G4) which is shown in Figure: (13) was used in this work for pin wear and disc roughness and wear measurements.

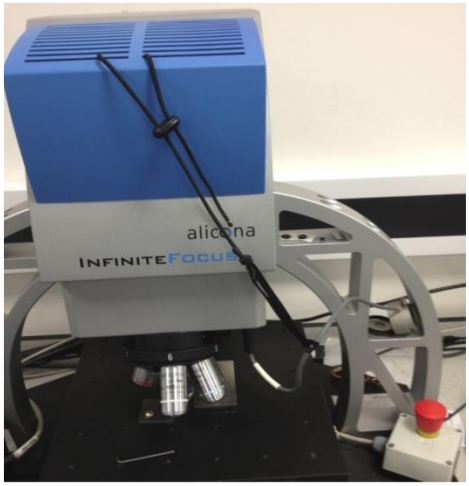

Figure: 13 Alicona (INFINTE FOCUS G4) [15]

Figure 14 shows a sample of the rail wear measurement using the Alicona profilometer which was carried out in this paper using the twin disc rig.

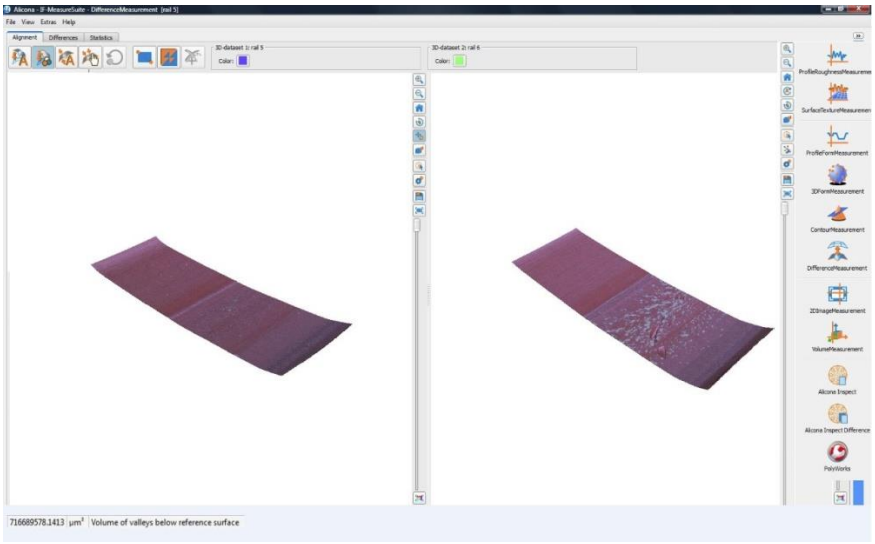

Figure: 14 Rail sample measurements using Alicona profilometer

Figure 15 shows a sample of replica surface for wheel under the lens of the Alicona profilometer. The sample dimensions were 5mm width and 35mm length; the roughness profile was shown in this Figure.

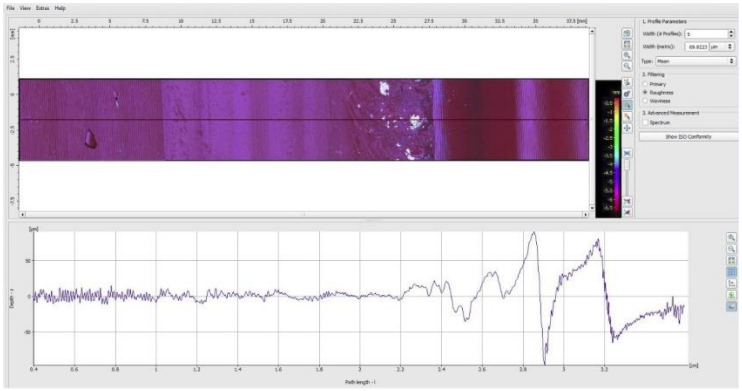

Figure: 15 Sample of replica of wheel profile under the Alicona profilometer

Figure 16 shows a sample of replica surface for rail under the lens of the Alicona profilometer. The sample dimensions were 5mm width and 20mm length; the roughness profile was shown in this Figure.

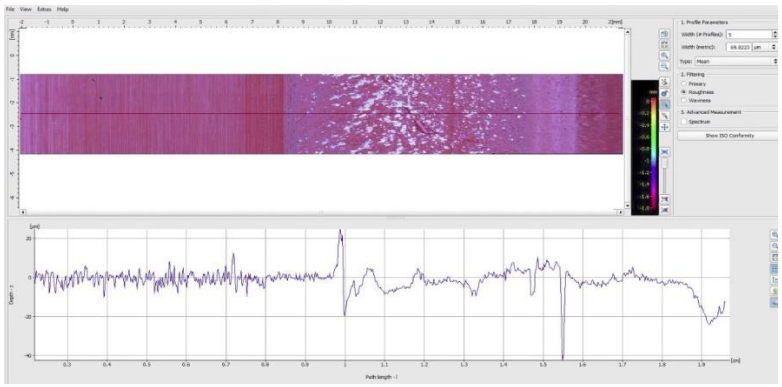

Figure: 16 Sample of replica of rail profile under the Alicona profilometer

4. Wheel/rail wear, and wheel/rail roughness measurements

In this work, several tests for wheel/rail wear, and wheel/rail roughness measurement using the twin disc rig, and Alicona profilometer were carried out under several conditions such as:

Effect of load on wheel/rail wear, and wheel/rail roughness over fixed time; such as in Table (1); under dry condition. (Speed =960rpm, test time = 60 min, and yaw angle = 0.4°). Table (1) shows the arithmetic average roughness and wheel/rail wear for wheel and rail after applying different values of load. The arithmetic average roughness and wear were measured using the Alicona profilometer.

Table 1 Effect of load on wheel/rail wear and Ra

No	Load (N)	Wheel wear (mm^3)	Rail wear (mm^3)	R_a for w (μm)	R_a for r (μm)
1	1000	1.1886	0.7166	3.5371	2.1232
2	1400	2.1225	1.3221	4.0957	3.8251
3	1800	3.6387	2.3639	4.3696	4.2429
4	2200	4.3870	3.4815	4.8643	4.6598
5	2600	5.8493	4.8744	5.1319	5.0726
6	3000	6.6227	5.3814	5.2357	5.1158
7	3400	8.9447	7.5931	5.6357	5.4151

Figure 17 shows the variation of arithmetic average roughness (R_a) with different values of load for wheel/rail surfaces.

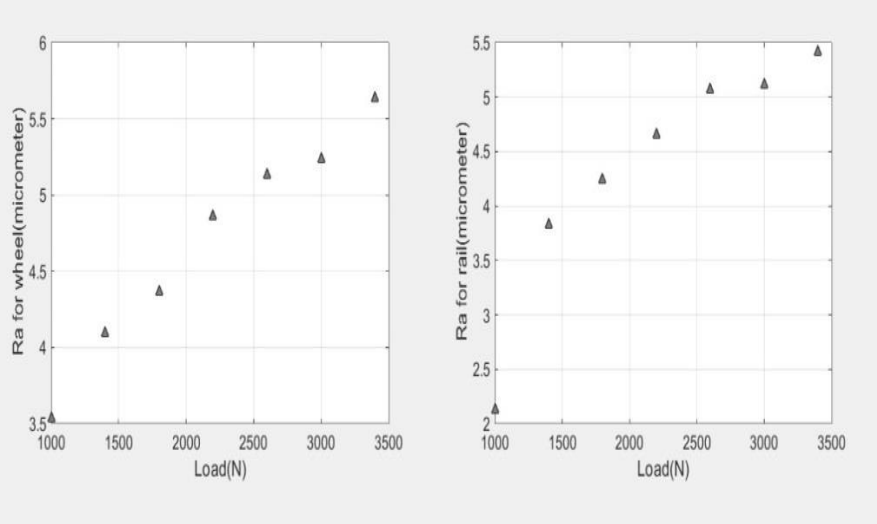

Figure: 17 Variation of arithmetic average roughness (R_a) with different values of load.

Effect of yaw angle on wheel/rail wear, and wheel/rail roughness over fixed time; such as in Table (2); under dry condition. (Speed =960rpm, load 2200N, and test time = 60 min). Table (2) shows the arithmetic average roughness and wheel/rail wear for wheel and rail after applying different values of yaw angle. The arithmetic average roughness and wear were measured using the Alicona profilometer.

Table 2 Effect of yaw angle on wheel/rail wear and Ra

No	Yaw angle (degree)	Wheel wear (mm^3)	Rail wear (mm^3)	R_a for w (μm)	R_a for r (μm)
1	0.1	1.2351	1.1721	2.6459	2.3576
2	0.2	1.6765	1.6265	3.1597	2.8613
3	0.3	2.1225	3.0609	3.2085	3.4548
4	0.4	3.1702	3.6511	3.9405	3.6072
5	0.5	5.8254	4.6919	5.4428	4.1522
6	0.6	7.4042	7.216	6.9407	5.8913
7	0.7	9.2830	8.7792	7.4647	7.2941

Figure 18 shows the variation of arithmetic average roughness (R_a) with different values of yaw angle for wheel and rail surfaces.

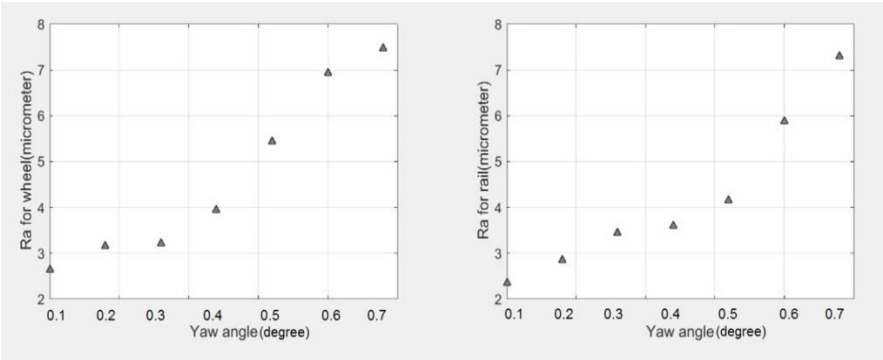

Figure: 18 Variation of arithmetic average roughness (R_a) with different values of yaw angle

Effect of speed on wheel/rail wear, and wheel/rail roughness over fixed time over fixed time under dry condition with different values of speed, such as in Table (3). (Load =1000N, and yaw angle = 0.1°, and test time = 10 min). Table (3) shows the arithmetic average roughness and wheel/rail wear for wheel and rail after applying different values of speed. The arithmetic average roughness and wear were measured using the Alicona profilometer.

Table 3 Effect of speed on wheel/rail wear and Ra

No	Speed (rpm)	Wheel wear (mm^3)	Rail wear (mm^3)	R_a for (μm)	R_a for (μm)
1	300	0.0823	0.0769	1.1062	1.0742
2	420	0.1997	0.1646	1.3783	1.2202
3	540	0.3668	0.3405	1.6430	1.4360
4	660	0.4536	0.4104	1.9292	1.8075

Figure 19 shows the variation of arithmetic average roughness (R_a) with different values of speed for wheel and rail surfaces.

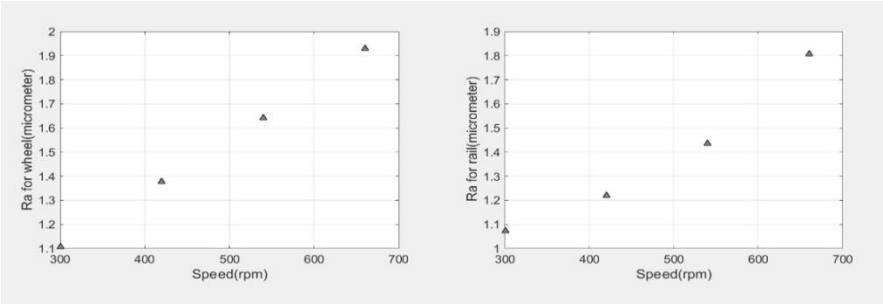

Figure: 19 Variation of arithmetic average roughness (R_a) with different values of speed

5. Conclusion

Several tests were carried out using the twin disc rig machine, and then, these measurements were used to establish how the relation between the wheel/rail surface roughness parameters and the wheel/rail wear. This work presented that the wheel/rail wear and roughness can be measured using and replica material and Alicona profilometer. For wheel/rail wear measurements, the replica material applied to the wheel/rail surfaces of the twin test rig to make a copy of both surfaces, then, the replica samples were scanned using an optical profilometer and the results were processed to establish wheel/rail wear and roughness parameter. The relation between wheel/rail wear and wheel/rail roughness parameter under different of load, yaw angle and speed were investigated. Test results show that the relation between the wheel/rail surface roughness parameter and wheel/rail wear, when the arithmetic average roughness R_a increased, as a result, the wheel/rail wear occurred faster in case of change of load, yaw angle, and speed. The arithmetic average roughness of wheel/rail, and the wheel/rail wear were bigger in case of change of yaw angle, it was bigger than the cases of change of load and speed, that because of the contact was closed to the flange rather than the tread in case of yaw angle tests.

References

[1] V. Bellitto, ATOMIC FORCE MICROSCOPY IMAGING, MEASURING AND MANIPULATING SURFACES AT THE ATOMIC SCALE. Croatia, 2012.

[2] B. Bhushan, Introduction to tribology: John Wiley & Sons, 2013.

[3] S. Tavares, "Analysis of surface roughness and models of mechanical contacts," University of Pisa, 2005.

[4] B. Bhushan, Modern Tribology Handbook, Two Volume Set: Crc Press, 2000.

[5] B. Muralikrishnan and J. Raja, Computational surface and roundness metrology: Springer Science & Business Media, 2008.

[6] U. Khandey, "Optimization of surface roughness, material removal rate and cutting tool flank wear in turning using extended taguchi approach," Master thesis, National institute of technology India, 2009.

[7] "Surface Metrology Guide - Surfaces and Profiles," http://www.htskorea.com/tech/spm/profile.pdf.2015

[8] Z. Dimkovski, "Characterization of a Cylinder Liner Surface by Roughness Parameters Analysis," Blekinge Institute of Technology, Karlskrona, Sweden, 2006.

[9] J. K. Brennan, "Algorithms for surface texture profiles and parameters," University of Huddersfield, 2010.

[10] S. Srirattayawong, "CFD study of surface roughness effects on the thermo-elastohydrodynamic lubrication line contact problem," Department of Engineering, 2014.

[11] a. J. R. T. V. Vorburger, "Surface Finish Metroology Tutorial," USA1990.

[12] N. Bosso and N. Zampieri, "Experimental and numerical simulation of wheel-rail adhesion and wear using a scaled roller rig and a real-time contact code," Shock and Vibration, vol. 2014, 2014.

[13] E. Gallardo-Hernandez and R. Lewis, "Twin disc assessment of wheel/rail adhesion," Wear, vol. 265, pp. 1309-1316, 2008.

[14] R. Lewis, R. Dwyer-Joyce, U. Olofsson, and R. Hallam, "Wheel material wear mechanisms and transitions," 2004.

[15] A. Shebani, "PREDICTION OF WHEEL AND RAIL WEAR USING ARTIFICIAL NEURAL NETWORKS," PhD, Computing and Engineering, University of Huddersfield UK, 2017.

[16] Alicona, Optical 3D micro coordiate measurement from & roughness vol. Version 3.9.1 EN 2011.